

Article

A Practical Disturbance Rejection Control Scheme for Permanent Magnet Synchronous Motors

Kanat Suleimenov  and Ton Duc Do * 

Department of Robotics, School of Engineering and Digital Sciences (SEDS), Nazarbayev University, Nur-Sultan Z05H0P9, Kazakhstan

* Correspondence: doduc.ton@nu.edu.kz

Abstract: This paper proposes a novel disturbance rejection control scheme for permanent magnet synchronous motor (PMSM) drives. Based on the framework of modified disturbance observer (DOB)-based control, the final topology of the proposed disturbance rejection proportional–integral (DR-PI) controller includes a pre-filter and a controller in a proportional–integral (PI) form. The proposed DR-PI control scheme is practical with a straightforward gain tuning rule. Note that the gain selection method is the main issue of not only conventional PI controllers but also advanced methods such as DOB-based controllers. In addition, by starting from the framework of modified DOB, this paper also proves that the PI controller with an pre-filter possesses a disturbance rejection ability similar to a DOB-based control method. To the best of our knowledge, this is the first time that such a simple and effective PI controller is designed for the speed control of PMSMs as well as theoretically proven to have a perfect disturbance rejection ability. This paper shows the steps of selecting the parameters of the proposed controller in terms of the parameters of a desired plant model, disturbance observer and compensator. Hence, unlike a traditional DOB case, in this approach, one can simultaneously tune the controller and observer at the same time. The appearance of the pre-filter from the modified DOB scheme solves an overshoot problem, thus the general motor operation is significantly improved, which is validated by experiments. The experimental evidence under two scenarios of load torque change and speed change prove the effectiveness of the proposed method compared to conventional PI and DOB control (DOBC) schemes. All the experiments were implemented on a 300 W PMSM of a setup manufactured by Lucas-Nuelle GmbH with a digital signal processor.

Keywords: disturbance rejection control; disturbance observer; permanent magnet synchronous motor (PMSM); proportional–integral (PI) control; speed control



Citation: Suleimenov, K.; Do, T.D. A Practical Disturbance Rejection Control Scheme for Permanent Magnet Synchronous Motors. *Symmetry* **2022**, *14*, 1873. <https://doi.org/10.3390/sym14091873>

Academic Editors: Shyh-Chour Huang and Jan Awrejcewicz

Received: 2 August 2022

Accepted: 31 August 2022

Published: 8 September 2022

Publisher's Note: MDPI stays neutral with regard to jurisdictional claims in published maps and institutional affiliations.



Copyright: © 2022 by the authors. Licensee MDPI, Basel, Switzerland. This article is an open access article distributed under the terms and conditions of the Creative Commons Attribution (CC BY) license (<https://creativecommons.org/licenses/by/4.0/>).

1. Introduction

Thanks to its advantages including its high efficiency, compact size, high torque-to-current ratio, high reliability, and recent advancements in permanent magnet (PM) materials, permanent magnet synchronous motors (PMSMs) have become increasingly popular among other types of AC drives [1–5]. Three classes of PMs such as alnico (alloy of aluminum, nickel, cobalt, iron, and other elements), ferrites, and rare-earth elements (neodymium–iron–boron (NdFeB), samarium–cobalt (SmCo)) are utilized in electrical drives [6,7]. Precisely controlling the PMSMs is generally challenging task due to their non-linear characteristics and various sources of disturbance noises such as external load torque, frictions, and sensor noises [8]. The conventional proportional–integral (PI) controller is widely applied for electrical drives including PMSMs because of its simple structure compared to existing advanced control solutions. Moreover, the PI controller has a disturbance compensation property inside of its control structure, i.e., it takes the tracking error in a speed loop to estimate an offset as well as the external disturbance to compensate [9,10]. In speed tracking problems of PMSMs, PI controllers are utilized in cascaded form, i.e., one

PI controller for the outer speed loop and two PI controllers for the inner current loop. It is claimed that, under the effect of disturbance, an output of the speed controller could cause the improper reference for the i_q -current controller, which in turn leads to degrading the PMSM's performance [11]. Moreover, this also reveals that there is a lack of detailed analysis about the mechanism of disturbance rejection in practical PI controllers [12]. On the other hand, despite the linear and simple structure of the conventional PI controller, it is hard to find a consensus on the rules for tuning the controller parameters. Most famous tuning techniques require a precise plant model, which often prevents the designer choosing appropriate gains for their applications [13].

For most industrial control systems, the performance of disturbance rejection is more vital than the perfect reference point tracking performance [10]. A large number of control solutions with disturbance rejection mechanisms [14–25] are introduced for the high performance control of PMSM drives. In [14], the extended state observer (ESO) was used to design a so-called linear–nonlinear switching active disturbance rejection control (ADRC) for the speed and current control loops of a PMSM. The main advantage of this method is that it integrates both the linear ESO and the nonlinear ESO to improve the conventional ESO. Another switching ADRC was introduced for PMSMs in [22]. According to this paper, the linear ESO is designed to estimate large disturbances, while the nonlinear ESO estimates small disturbances. The parameters of the linear ESO are tuned by using the frequency domain analysis, whereas the parameter tuning of the nonlinear ESO is still based on the practical experience. A DOB-based controller (DOBC) is utilized for estimating unmatched disturbances in PMSMs [15]. The contribution of this paper is the integration of the current-constrained proportional–integral–derivative (PID) with an observer. According to the results in [13], it can be seen that the conventional DOBC shows a good disturbance rejection ability with some small violation in the current constraint. A high-order disturbance observer is used with the suboptimal speed controller in [16] to improve the robustness of an interior PMSM (IPMSM). In this work, the conventional assumption about slowly varying disturbance is released. Whilst it also shows satisfactory results, however, the general implementation of the method might require high-performance processors. The enhancement of linear active disturbance rejection control (LADRC) was successfully introduced for PMSM in [15]. Two linear extended state observers (LESOs) work together to estimate external and internal disturbances. An application of a special PIDs coined fractional-order PID (FOPID) and fractional-order PI (FOPI) for PMSMs were studied in [19,20]. In [19], the parameters of the FOPID were determined using optimization algorithms, whereas in [20], a nonlinear disturbance observer (NLDO) estimated a load torque and the FOPI adjusted its parameters online based on the a algorithm. However, to use the FOPI, the plant model should first be linearized. The work in [21] presented an application of ESO-based internal model control (IMC)-PID for permanent magnet linear synchronous motors (PMLSMs). Although the control scheme in [21] showed better results comparing to conventional ones, the parameters of the IMC-PID can only be obtained when there is available information about the plant. Hence, the model identification technique should be used to calculate the nominal values of a plant. An augmented observer in [23] was designed to estimate the disturbances coming from multiple sources in PMSM drives. Although the designed control scheme is able to suppress multiple disturbances, the tuning procedures of the controller and observer parameters are not clearly shown. The first-order LADRC in [24] was implemented for a five-phase PMSM. The method of feedback linearization and extended high-gain observer in [25] was proposed for the speed control of PMSMs. Although the speed response of the method was better than that of the traditional PI, detailed steps on observer design and results of disturbance estimation are missed. In [26], a sliding-mode observer was presented to estimate the rotor position. In that paper, the harmonics in the back electromotive force (EMF) was filtered out by a multi-proportional resonant filter instead of a low-pass filter. The rotor position estimation method presented in [27] utilizes a dual Luenberger observer. The general structure of the control system in [27] is based on the cascaded PI-PI control scheme. A composite nonlinear speed controller was proposed

in [28] to regulate the speed of a PMSM. This method is based on the ESO design, and it showed satisfactory simulation results, however, more experimental studies should be performed to validate the practicality of the proposed method. Fuzzy logic was used in [29] to design a fuzzy adaptive repetitive speed controller for PMSMs. Fuzzy logic-based sliding mode speed control for a PMSM was presented in [30]. The fuzzy algorithm was added to solve a problem with chattering phenomena during steady states as well as to improve the transient performance of the control system.

In this paper, a novel disturbance rejection PI (DR-PI) control algorithm was introduced for the speed regulation of PMSMs. The main objective of this study was to prove the perfect disturbance rejection of a PI controller with a pre-filter and a practical tuning method for the parameters of a PI controller based on the modified DOBC framework. Instead of separately designing a disturbance observer and then compensating it in the PI speed controller, the observer and PI controller are combined in a compact structure, called DR-PI. With this form and its root from the modified DOBC, the gain tuning becomes straightforward and thus practical. Moreover, in our design, the common issues with the overshoot of conventional PI control are eliminated via the good design of the pre-filter of the proposed DR-PI. The experimental evidence shows that the proposed design is not only simpler than the DOBC, but also achieves certain advantages during transient time. In summary, the contributions of this work are as follows: (1) A novel disturbance rejection control scheme for PMSMs: in a conventional PI controller, it is not straightforward to determine the relationship between the controller parameters and system response. In recent works, one needs to have the known model of a process to tune the PI controller. The Ziegler–Nichols (ZN) tuning method is one of the most popular methods used for tuning PI controllers. However, the ZN method is considered an empiric one, and in practice, the controller gains tuned by the ZN method might result in unsatisfactory performance. Furthermore, it is difficult to establish stability conditions using the ZN tuning method. Considering these facts, it was stated in [12] that, within the modified DOBC framework, only rough information such as the order of the plant is enough to design a disturbance rejection controller. Therefore, in this paper, based on the modified DOBC scheme, a PI controller with a pre-filter is designed with a clearly defined relationship of the controller parameters and the process through the time constants of the Q-filter and the desired closed-loop model. To the best of our knowledge, this is the first study to design a compact DR-PI to effectively control a PMSM; (2) A practical tuning process of the PI controller to deal with the external disturbances of PMSMs: with a simple but effective structure, the gain tuning process becomes very straightforward. The explicit form of the DR-PI makes the stability analysis and the gain selection procedure extremely simple; (3) A useful design in which the nominal parameters are not required: in this paper, we introduce the desired closed-loop model of a plant, and consequently avoid the requirement for knowledge of the nominal parameters; (4) Finally, the simple topology and the implementation of the pre-filter help eliminate an overshoot, which is common for a conventional PI scheme tuned by the ZN or other methods.

2. Problem Formulation

2.1. Preliminary

Any plant to be controlled must satisfy the minimum phase (MP) condition in order to guarantee satisfactory control performance. Most industrial plants are MP systems with a relatively low order. Hence, a large number of research studies have investigated such systems [12]. In this study, we assume that the current controllers are properly tuned and hence, the objective is to design a PI speed controller with an enhanced disturbance rejection mechanism.

In this study, we assume that the real plant $P(s)$ and nominal plant $P_n(s)$ are in the set of uncertain plants Γ [10,24].

$$\Gamma = \left\{ \begin{array}{l} P(s) = \frac{\rho_{n-k}s^{n-k} + \rho_{n-k-1}s^{n-k-1} + \dots + \rho_0}{\lambda_n s^n + \lambda_{n-1}s^{n-1} + \dots + \lambda_0} \\ : \lambda_l \in [\lambda_l^-, \lambda_l^+], \rho_l \in [\rho_l^-, \rho_l^+] \end{array} \right\} \quad (1)$$

in which n and k are defined as positive integers and $n \geq k$; $\lambda_i^-, \lambda_i^+, \rho_i^-, \rho_i^+$ are known constants which define the intervals $[\lambda_n^-, \lambda_n^+] \subset (0, \infty)$ and $[\rho_{n-k}^-, \rho_{n-k}^+] \subset (0, \infty)$. This means that the given intervals do not include zero, hence the relative order of $P(s)$ is not changed. Note that the relative order of $P(s)$ is defined by k and the set Γ is determined to be sufficiently large with bounded parametric uncertainties.

2.2. Dynamic Model

It is well known that the response of mechanical rotor speed ω_m is due to the interaction of the mechanical torque T_m and the external load torque T_l , which can be explained by the equation:

$$J_m \dot{\omega}_m = T_m - T_l \quad (2)$$

where J_m is the rotor inertia. On the other hand, the mechanical torque T_m can be expressed as

$$T_m = T_e - T_{fr} - T_{vs} - T_{flux};$$

$$T_{fr} = (b_{hys} + b_{fr}) \text{sign}(\omega_m);$$

$$T_{vs} = (b_{ed} + d_{vs}) \omega_m;$$

$$T_{flux} = c_{ed} \frac{\frac{d\psi}{dt} \times \psi}{|\Phi_{dq}|^2};$$

where T_e : electromagnetic torque; T_{fr} : a friction torque; T_{vs} : viscous torque; and T_{flux} : torque due to the pulling force of flux with b_{hys} , b_{ed} , and b_{fr} for the hysteresis loss coefficient, an Eddy current coefficient, and a static friction constant, respectively; ψ is a magnetic flux linkage; and c_{ed} is an Eddy current damping coefficient. Hence, (2) can be modified as follows

$$J_m \dot{\omega}_m = T_e - T_{fr} - T_{vs} - T_{flux} - T_l = T_e - z \quad (3)$$

where z represents a total disturbance and it is a sum of all the torques described above— $z = T_l + T_{fr} + T_{vs} + T_{flux}$.

Assumption 1. (1) The mechanical rotor speed ω_m is available; (2) T_l , T_{fr} , T_{vs} , T_{flux} are unknown.

Remark 1. In numerous publications, such as [14,15,20,22,25,31,32], the total disturbance z in (3) only has two terms: T_{vs} and T_l , where T_{vs} is given as a linear functions of rotor speed with a known negative coefficient. Such modeling has two main problems: (1) It is impractical to model the T_{vs} and determine its coefficient(s); and (2) Other disturbances such as T_{fr} and T_{flux} are omitted, which is not reflected the real practice.

Equation (3) represents a first-order system with disturbance and its transfer function is

$$P(s) = \frac{1}{J_m s} \quad (4)$$

This plant belongs to the set shown in (1) and with the low relative order, i.e., first order. In this system, ω_m represents the system output whereas an electromagnetic torque T_e defines the control input.

The system in (3) can be represented in the following general form in the frequency domain,

$$Y(s) = P(s)(U(s) + Z(s)) \quad (5)$$

in which $Y(s)$, $U(s)$, and $Z(s)$ are the plant output, the control input, and the disturbance in the frequency domain, respectively. In this case, $Y = \omega_m$ and $U = T_e$. For simplicity, we omit the s -variable in the signal notations.

3. Design of Disturbance Rejection Control Scheme for PMSMs

3.1. Disturbance Rejection Control

To reject the disturbance, a DOBC need to be designed. There are many variations of DOBCs. Figure 1 represents the block diagram of one modified DOBC. In this figure, $R(s)$ is the speed reference and W_r is the estimated function of the plant. The modified disturbance observer reported in [33] uses the inverse of W_r , i.e., W_r^{-1} , instead of P_n^{-1} , which is used in the conventional DOBC scheme. This modification helps solve the problem with unstable poles and the canceling of zeros. Introducing a compensator K such that $U = KU_d$ and modifying (5) gives

$$Y = W_r U_d + (PK - W_r)U_d + PZ = W_r(U_d + \zeta) \quad (6)$$

in which $\zeta = \zeta_1 + \zeta_2$, $\zeta_1 = W_r^{-1}(PK - W_r)U_d$, and $\zeta_2 = W_r^{-1}PZ$. ζ_1 and ζ_2 are internal and external disturbances, respectively. These two terms define a total disturbance ζ . As shown, ζ_1 exists due to $(PK - W_r)$ and a large difference creates a large ζ_1 . A large ζ_1 negatively affects the transient performance and the system's stability.

Remark 2. In the conventional DOBC scheme, the main difficulties lie in determination of $P_n^{-1}P$, which in turn creates limitations on the stability and performance of a system. In addition, the nominal parameters need to be known. Therefore, the main idea in [13,33] is to introduce a stable and minimum-phase (MP) transfer function W_r with a tunable and desired performance instead of nominal plant P_n . Hence, the limitations of the DOBC are solved and its application is broadened.

A low pass Q-filter has a fractional rational form

$$Q(s) = \frac{w_{m-k}(\eta s)^p + w_{m-k-1}(\eta s)^{p-1} + \dots + w_0}{(\eta s)^m + x_{m-1}(\eta s)^{m-1} + \dots + x_0} \quad (7)$$

where $\eta > 0$ is a time constant which defines a bandwidth of the Q-filter; p, m are non-negative integers satisfying $p \leq m - \text{rel.deg}(W_r)$ and are chosen such that they have a proper and realizable QW_r^{-1} , whereas the parameters of the characteristic equation of the Q-filter are chosen such that $(\eta s)^m + x_{m-1}(\eta s)^{m-1} + \dots + x_0$ is Hurwitz stable and $\frac{w_0}{x_0} = 1$.

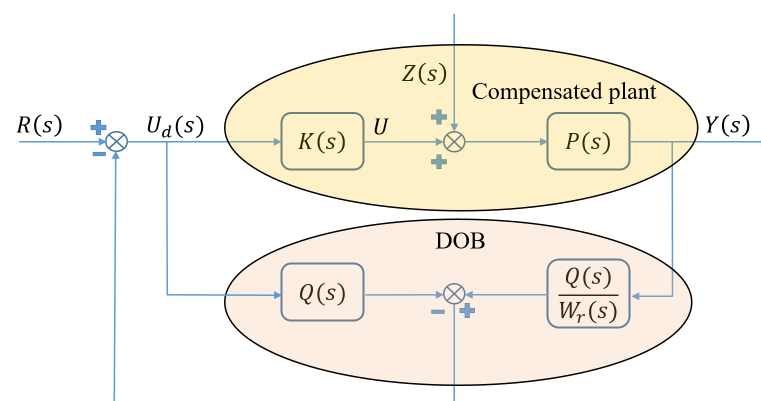


Figure 1. Modified DOB scheme.

The desired MP model for the plant is given as a first-order transfer function

$$W_r = \frac{1}{\mu s + 1} \quad (8)$$

Remark 3. Note that the proposed method is applicable for systems with a maximum relative degree of 2. From (4), it is revealed that the relative degree of the speed loop is 1. From the modified DOB in Figure 1, we can select a compensator K such that the compensated plant $P(s)K(s)$ has a relative degree equal to 1. Recall that the external disturbances ζ_1 in (6) are created due to $(PK - W_r)$. Therefore, in order to match the order between the compensated plant and desired plant W_r , we can choose the desired model W_r as shown in (8).

The compensator has a form $K(s) = k_c(\sigma s + 1)$, in which $k_c > 0$ and $\sigma \geq 0$. The parameter σ is used for the phase-lead compensation of the plant $P(s)$. The value of the k_c is obtained such that obtaining a stable open-loop $P(s)K(s)$ and its value depends on the existence of right-half plane (RHP) zeros or poles, as shown below

$$\begin{cases} k_c = \frac{\lambda_n}{\rho_{n-k}H}, & \text{if no zeros on RHP} \\ k_c = \frac{\lambda_0}{\rho_0}, & \text{if no poles on RHP} \end{cases} \quad (9)$$

Remark 4. For the plants with slow dynamics and a large μ , a large σ should be set. In contrast, for the plants with fast dynamics and small μ , a small σ should be defined.

Based on the modified DOBC in Figure 1, a closed-loop transfer function for the control system is derived as

$$G = \frac{KW_rP}{KQP + W_r - W_rQ} \quad (10)$$

It should be noted that the closed-loop transfer function of the proposed DR-PI controller-based system is similar to (10). It is known that the general transfer function of a negative unity-feedback closed-loop system is defined by $G' = \frac{P'K'}{1+P'K'}$, where P' and K' are a plant and controller, in general. To have (10) in the general form, let us divide the numerator and denominator of (10) by KQP , and hence

$$G = \frac{\frac{W_r}{Q}}{1 + \frac{W_r}{KQP} - \frac{W_r}{KP}} = \frac{\frac{W_r}{Q}}{1 + \frac{W_r - W_rQ}{KQP}} \quad (11)$$

Then, after some mathematical manipulations, (11) can be written as

$$G = \frac{\frac{W_r}{Q} \frac{KQP}{W_r - W_rQ}}{1 + \frac{KQP}{W_r - W_rQ}} \quad (12)$$

Noting that $G = \frac{Y}{R}$, (12) is modified as

$$\frac{Y}{R \frac{W_r}{Q}} = \frac{\frac{KQP}{W_r - W_rQ}}{1 + \frac{KQP}{W_r - W_rQ}} \quad (13)$$

Hence, from (13), it is obtained that the proposed controller derived from the modified DOBC scheme should have a form

$$C_{DR-PI} = \frac{K(s)Q(s)}{W_r(s)(1 - Q(s))} \quad (14)$$

The DR-PI diagram is proposed as shown in Figure 2. $\frac{W_r(s)}{Q(s)}$ in (13) corresponds to a pre-filter of the reference signal.

After the substitution of $W_r(s)$, $Q(s)$, and $K(s)$ into (14), the DR-PI is obtained

$$\begin{cases} C_{DR-PI} = \frac{\lambda_n}{\rho_{n-k}\eta} + \frac{\lambda_n}{\rho_{n-k}\eta\mu s}, & \text{if no zeros on RHP} \\ C_{DR-PI} = \frac{\lambda_0}{\rho_0\eta\mu} + \frac{\lambda_0}{\rho_0\eta s}, & \text{if no poles on RHP} \end{cases} \quad (15)$$

The pre-filter in (13) is chosen in the form as in [11].

$$S_r(s) = \frac{\alpha\mu}{\mu s + \alpha} \quad (16)$$

Furthermore, the Q-filter in (7) is taken as a first-order transfer function

$$Q(s) = \frac{1}{\eta s + 1} \quad (17)$$

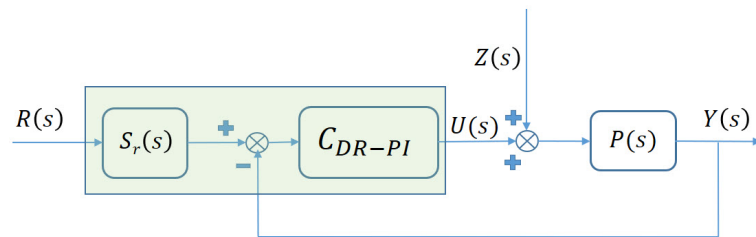


Figure 2. Proposed DR-PI controller.

3.2. Disturbance Rejection Control for PMSMs

From (4), it can be seen that we have a first-order transfer function in the speed loop. The obtained transfer function has no zeros on the RHP and has a pole with real and imaginary parts, both equal to zero. Hence, we consider a case in which there are no zeros on the RHP and set $n = 1$, $k = 1$ to define k_c from (9) and DR-PI in (15) as $k_c = \frac{\lambda_1}{\rho_0\mu}$ and $C_{DR-PI} = \frac{\lambda_1}{\rho_0\eta} + \frac{\lambda_1}{\rho_0\eta\mu s}$. Let us write the DR-PI controller in the conventional structure as

$$C_{DR-PI} = K_p \left(1 + \frac{1}{\mu s} \right) \quad (18)$$

where $K_p = \frac{\lambda_1}{\rho_0\eta} = \frac{k_c\mu}{\eta}$. From (18), it can be seen that the proportional gain and integral time constant are expressed via k_c , μ , and η , which, in turn, explicitly shows the interconnection between W_r , $Q(s)$, and $K(s)$. This advantage helps tune the PI controller in a more systematic way rather than the trial-and-error approach as in conventional PI controllers.

Remark 5. In the proposed DR-PI controller, there is no estimation signal of disturbance, as in many DOBC methods [14,15,20,22,25,31,32]. This makes sense as here we care about the disturbance rejection ability of the control scheme, not the estimation of the disturbance itself. In this case, the disturbance observer and controller are combined in order to make the controller simpler and more practical to design.

Remark 6. It should be noted that, one important difference of the proposed DR-PI compared to the other methods, is the pre-filter added to filter the reference speed. This pre-filter appears from the modified DOBC scheme and is then further adapted for DR-PI. In [34], a second-order filter with fast dynamics was added to the reference speed. The paper claimed that, by doing this, they can make the speed response faster without further analysis. In our case, the so-called pre-filter is the first-order filter playing the same role. The interesting point is that this pre-filter is derived from the framework of a modified DOBC. A pre-filter is successfully implemented in control systems introduced in [35–38].

3.3. Gain Tuning Mechanism

What is interesting here is that the modified-based DR controller for the system in (3) is reduced to a simple PI controller, as shown in (18) with a pre-filter in (16) after the reference signal, as presented in Figure 2. Moreover, as shown in [12], the ADRC can be represented as a PID controller for general second-order systems. Then, the question here now is how

to tune the PI/PID gains to effectively reject the disturbance. We can see that the proposed DR-PI controller now has the gains expressed via k_c , μ , and η and α in (18).

3.3.1. Stability-Based Gain Selections

Using (18), we can easily derive the following characteristic equation of the closed-loop control using the proposed DR-PI controller

$$(\mu s + \alpha) \left(s^2 + \frac{k_c \mu}{J_m \eta} s + \frac{k_c}{J_m \eta} \right) = 0 \quad (19)$$

Then, we have the following comments: (1) When all the parameters are positive, the characteristic equation in (19) always has its roots on the left half of the complex plane, i.e., it is always stable; (2) To improve the stability margin, i.e., the real part of the roots which is far from the origin, $\frac{k_c \mu}{J_m \eta}$ must be as big as possible.

3.3.2. Gain Selections Based on the Meaning of Functions

(1) η in (17) is designed for a low-pass filter, and the filter performance is better if η is smaller; (2) The reciprocal value of μ is the bandwidth parameter determining the speed of the closed-loop response, then μ can be selected to be small; (3) By default, α in (16) is set to be one.

As the final form of the DR-PI controller is a PI controller with a pre-filter, the stability analysis is made very simple by selecting gains to stabilize the characteristic Equation (19). Note that the μ selection is also discussed in Remark 3. The gain tuning procedure for the proposed DR-PI is presented in Figure 3. The overall diagram of the proposed DR-PI-based control scheme for PMSMs is illustrated in Figure 4.

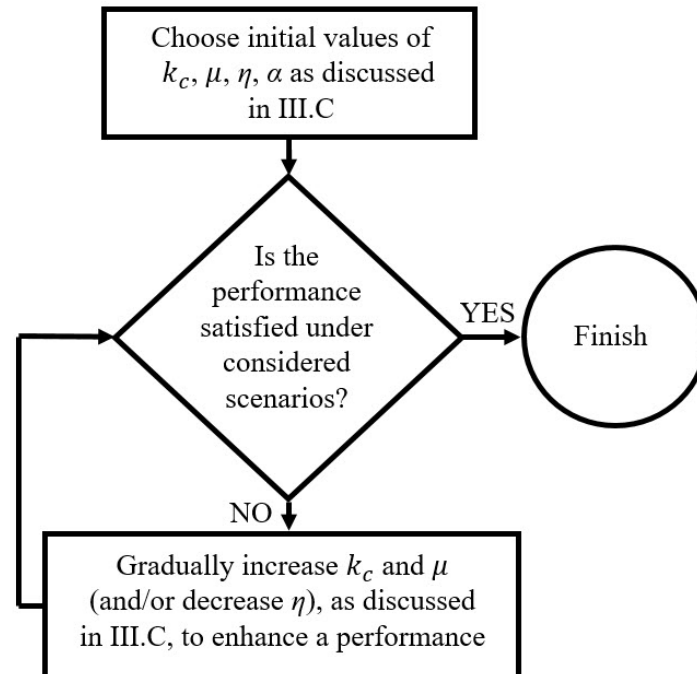


Figure 3. Tuning algorithm of the DR-PI.

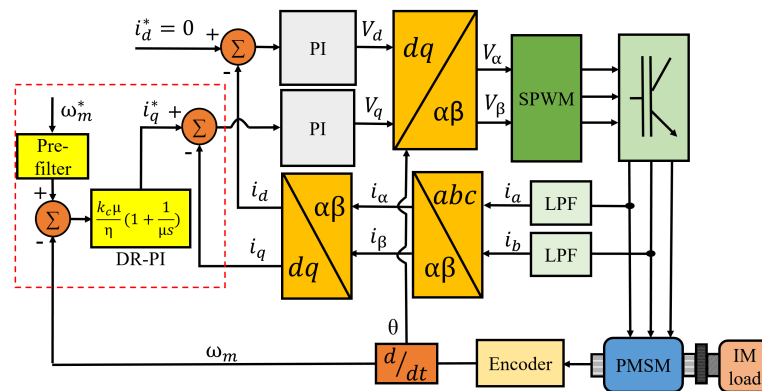


Figure 4. Overall diagram of the control system with the proposed DR-PI.

4. Results and Discussions

4.1. Simulations and Experiments Comparison

In the first part of the section, the simulation and experimental work are conducted to check the disturbance rejection performance of the proposed method with various controller gains. The simulations are performed on Matlab 2019a/Simulink environment and the experimental validations are based on a 300-W PMSM of a setup manufactured by Lucas-Nuelle GmbH (Figure 5). The load torque is supplied by a 1.7 KW induction motor (IM) controlled by the servo-machine control unit. The main control algorithm is prepared and tested in MATLAB 2019a/Simulink and processed with a 8 kHz digital signal processor (DSP). The PMSM parameters are given in Table 1. All the simulations and experiments are performed according to the scenarios presented in Figures 6 and 7.

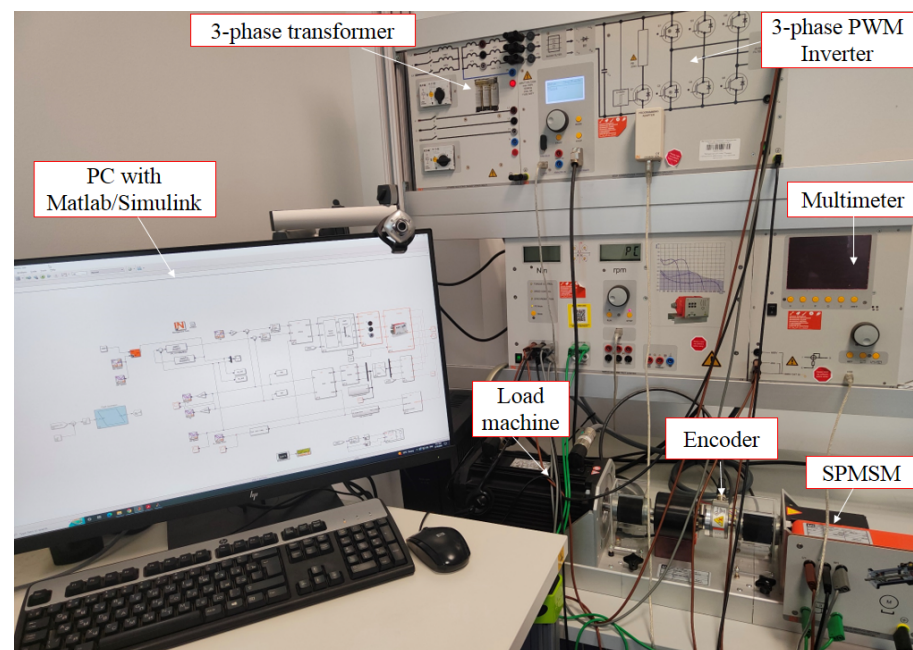


Figure 5. Experimental setup.

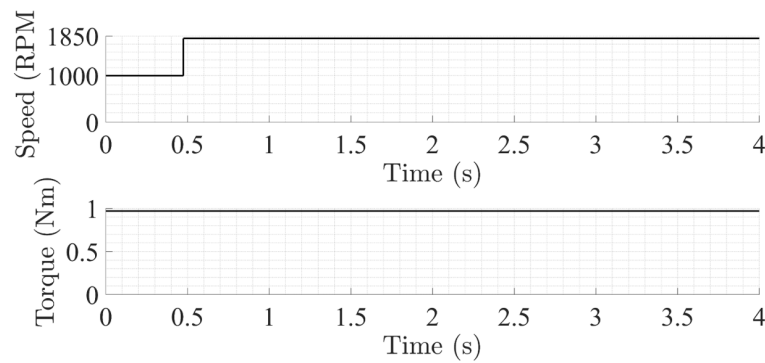


Figure 6. Step-change of the speed from 1000 rpm to 1800 rpm under the rated torque—Scenario 1.

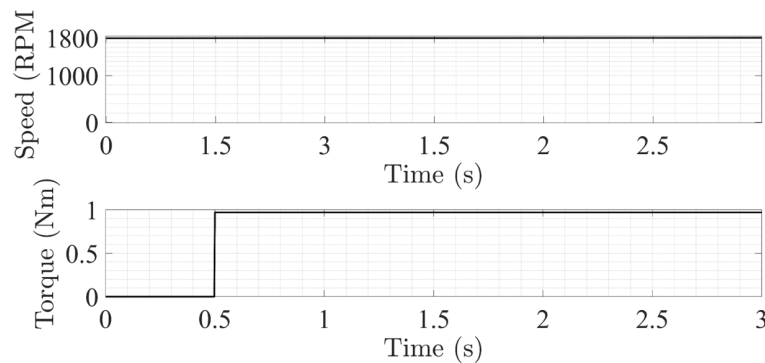


Figure 7. Step-change of the load torque from zero to a rated value at constant speed of 1800 rpm—Scenario 2.

Figure 8 shows the simulation result of the DR-PI controller when a rated load torque is suddenly applied at a constant speed of 1800 rpm (Scenario 2) with different values of proportional gains K_p . Four different proportional gains were tested which reveals that, with higher gains, the DR-PI performs with less drop and overshoot reference speed tracking. Figure 9 shows the current responses for each proportional gain in simulations for this case. On the other hand, Figures 10 and 11 illustrate the experimental results under the same conditions as simulation studies. This reveals that the performance of the system becomes better when the proportional gain is selected as close to 0.0495 as possible. We can also observe that the experimental results show the same trend as indicated by the simulations, although there are some detected differences. Tables The selected control gains of three methods are listed in Table 2. Tables 3 and 4 summarize the performance of the proposed controller associated with these simulation and experimental studies.

Table 1. Parameters of the PMSM.

Parameters	Values	Units
Rated speed, ω_{rated}	2500	rpm
Nominal load torque	0.97	N·m
Pole pairs, Z_p	4	-
Nominal resistance of the stator, R_s	2.37	Ω
Nominal inductance of the stator, L_s	4.3	m·H
Magnetic flux linkage, ϕ_m	0.0623	V·s/rad
Nominal inertia of the rotor, J_n	0.0033	kg·m ²

Table 2. Parameters of the speed controller.

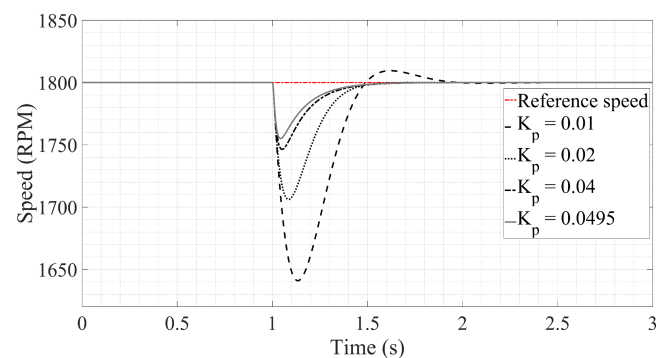
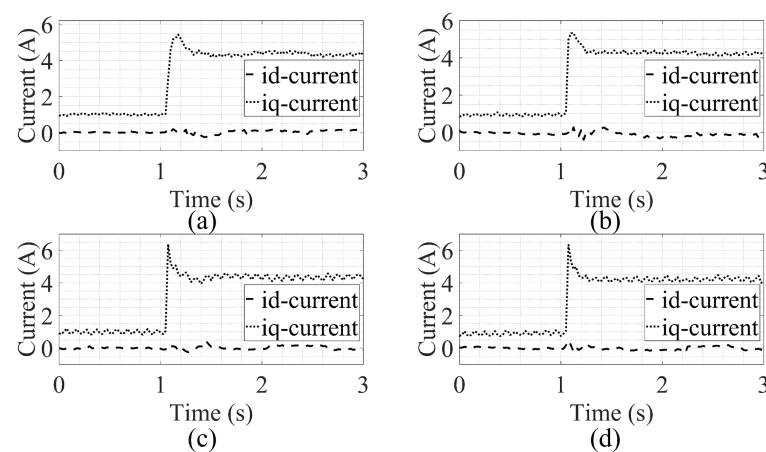
Parameter	Convent. PI	DOBC	DR-PI
Proportional gain, K_p	0.0045	0.0020	0.0495
Integral time constant, T_i	0.3000	0.0500	0.1500
Compensator gain, k_c	-	-	0.022
Time constant, η	-	-	0.0667
Time constant, μ	-	-	0.15

Table 3. Performance of DR-PI with a different K_p and constant $T_i = 0.15$ in simulations.

	$K_p = 0.01$	$K_p = 0.02$	$K_p = 0.04$	$K_p = 0.0495$
Speed overshoot, %	0.5	-	-	-
Speed drop, %	8.8	5.2	3	2.5

Table 4. Performance of DR-PI with a different K_p and constant $T_i = 0.15$ in experiments.

	$K_p = 0.01$	$K_p = 0.02$	$K_p = 0.04$	$K_p = 0.0495$
Speed overshoot, %	-	-	-	-
Speed drop, %	18	10	6.7	5.78

**Figure 8.** Speed response of the DR-PI with a different K_p and constant T_i under Scenario 2. Simulation result.**Figure 9.** Current response of the DR-PI with a different K_p and constant T_i under Scenario 2. Simulation result: (a) $K_p = 0.01$; (b) $K_p = 0.02$; (c) $K_p = 0.04$; and (d) $K_p = 0.0495$.

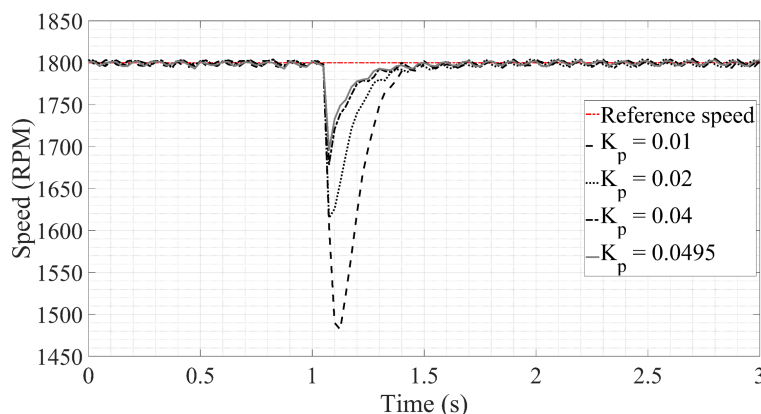


Figure 10. Speed response of the DR-PI with different K_p and constant T_i under Scenario 2. Experimental result.

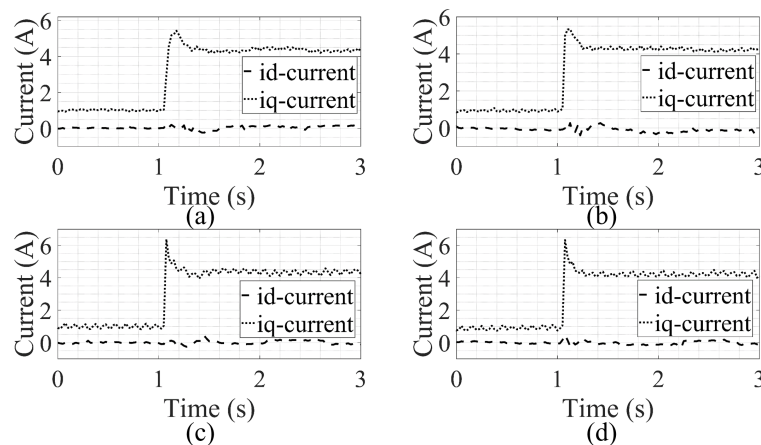


Figure 11. Current response of the DR-PI with different K_p and constant T_i under Scenario 2. Experimental result: (a) $K_p = 0.01$; (b) $K_p = 0.02$; (c) $K_p = 0.04$; and (d) $K_p = 0.0495$.

4.2. Comparative Experimental Results of the DR-PI, Conventional PI, and DOBC

In the second part of this section, the conventional PI and conventional DOBC schemes are compared experimentally with the proposed DR-PI. It is known that the ZN method provides the characteristics of a dynamic system based on its step response. The characteristics are mainly described in terms of the following parameters, the so-called ultimate period of oscillations T_{ult} , ultimate gain K_{ult} , and time delay D , or, shortly, $T_{ult}K_{ult}D$. In this study, the $T_{ult}K_{ult}D$ -based ZN [11] is utilized to find the gains of the conventional PI controller, whereas the gains of the PI in the DOBC are chosen by following the method in [33]. The $T_{ult}K_{ult}D$ values are found to be $T_{ult} = 0.15$ s, $K_{ult} = 303.0303$, and $D = 0.1$ s. Hence, the ZN-based conventional PI controller parameters are defined in terms of $T_{ult}K_{ult}D$ as below

$$K_p = \frac{0.9T}{K_{ult}D}$$

$$T_i = 3D$$

First, the performances of the controllers are analyzed under the constant rated load torque with a speed-change from 1000 rpm to 1800 rpm, i.e., Scenario 1 is presented in Figure 6. Figure 12 shows the speed responses of three controllers. From this plot, it is shown that even though the conventional PI and DOBC have a faster response in initial instances, the proposed DR-PI controller has the best tracking performance, i.e., it converges the fastest with the shortest settling time and no overshoot. Note that the conventional PI is better than DOBC with less settling time, i.e., 0.9 s/1.6 s, to reach and stay within a tolerance band of 1% at the steady state—whereas for the DR-PI, this value is 0.575 s.

Furthermore, the highest speed overshoot among three controllers belongs to the DOBC with a value of 5.56%, while the conventional PI and DR-PI, respectively, have values of 5.39% and 0%. This phenomenon is explained by the following reason: DOB is designed for disturbance rejection, however, it has some delays in the disturbance estimation and makes the speed response under the speed step-change condition worse than conventional PI. Furthermore, it is known that an overshoot negatively affects performance by elongating the settling time. The fast convergence of the proposed controller is mainly due to the appeared pre-filter based on the modified DOB which helps eliminate an overshoot and hence makes the overall DR-PI faster than the other two controllers. A fast convergence effect of a pre-filter can also be observed in the work of [34,39]. Figure 13 presents the associated dynamics of the i_d - and i_q -currents under this condition. The i_d -current for three controllers has a smooth shape and fluctuates around zero, however, the DR-PI can still maintain the i_d current better when the speed change occurs. The performance of three control methods are summarized in Figure 14.

In the second experiment, a step-change of load torque from zero to the rated value is applied when the constant reference speed is set to 1800 rpm (i.e., Scenario 2 shown in Figure 7). The speed responses of three controllers are presented in Figure 15. In this case, the proposed DR-PI significantly outperforms the two remaining controllers in terms of disturbance rejection ability. The maximum speed drop for the DR-PI case is approximately 4.33% compared to 10%/32.78% for the DOBC and conventional PI, respectively. At the same time, when the DOBC outputs an overshoot of 1.61%, both the conventional PI and DR-PI have no overshoot in speed response. Moreover, from Figure 15, it is observed that the DR-PI requires the shortest time to recover among three control methods (i.e., settling time, DR-PI: 0.2 s, DOBC: 1.05 s, conventional PI: 0.925 s). Note that the DOBC shows a superior disturbance rejection ability compared to the conventional PI control method (speed drop, DOBC: 10%, conventional PI: 32.78%) with a similar settling time (1.05 and 0.925 s), except for a small overshoot amount (1.61%). The advantages of both DOBC and DR-PI schemes can also be seen from the dynamics of the i_d - and i_q -currents shown in Figure 16. The DOBC and DR-PI controllers generate a quite similar i_q -current command, but the DR-PI has a sharp i_q -current shape when the rated torque is applied and it results in no overshoot and a small drop in speed response. Unlike the results of two other controllers, the conventional PI controller has the smoothest i_q meaning that this controller is not able withstand the sudden load changes and it requires more time to return to a steady state. In the DR-PI controller's case, the i_d -current fluctuates for approximately 0.2 s after the rated torque is applied, while the times for the conventional PI and DOBC are 1 s and 1.5 s, respectively. The speed regulation performance for Scenario 2 is illustrated in Figure 17.

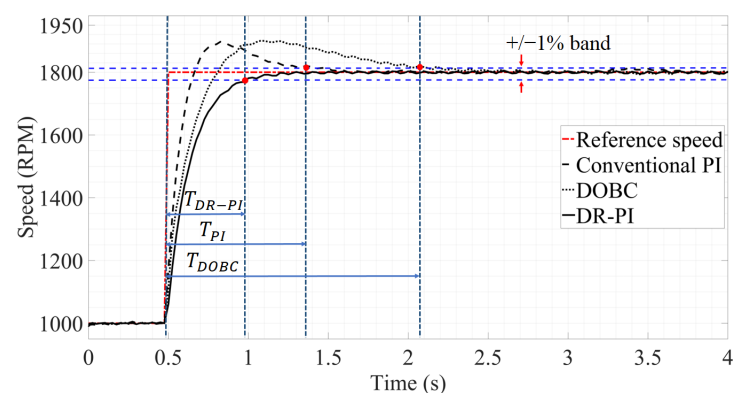


Figure 12. The speed responses of three control methods under Scenario 1.

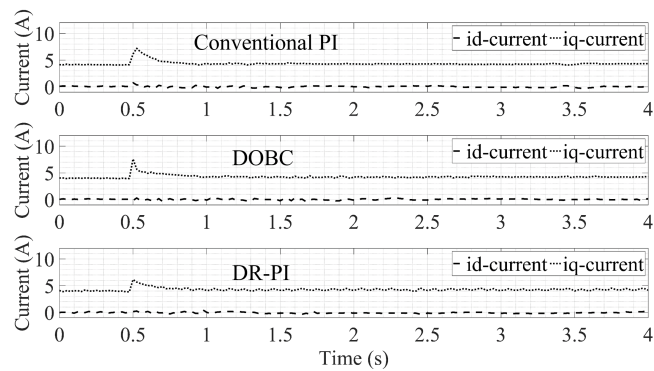


Figure 13. i_d and i_q currents dynamics of three control methods under Scenario 1.

The experimental results show that, compared to the conventional PI and DOBC schemes, the proposed DR-PI has the best disturbance rejection ability with the smoothest current shapes and shorter time for recovering after a disturbance effect.

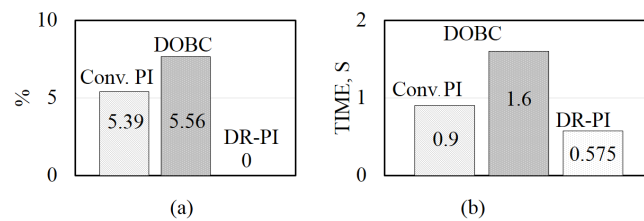


Figure 14. Numerical performance of three control methods under Scenario 1: (a) speed overshoot; and (b) settling time.

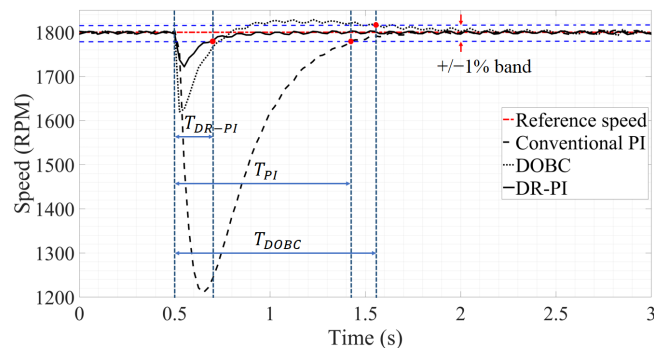


Figure 15. Speed tracking performances of three control methods under Scenario 2.

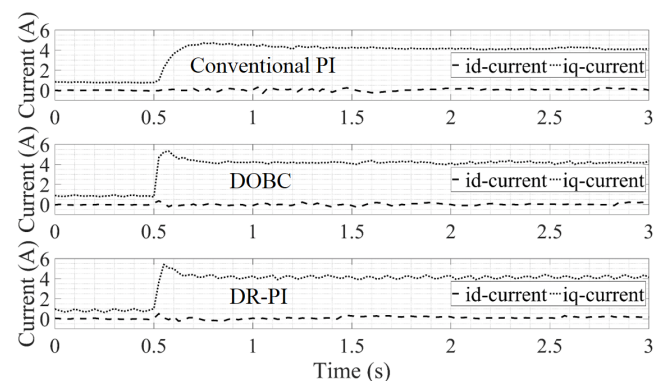


Figure 16. i_d and i_q currents of three control methods under Scenario 2.

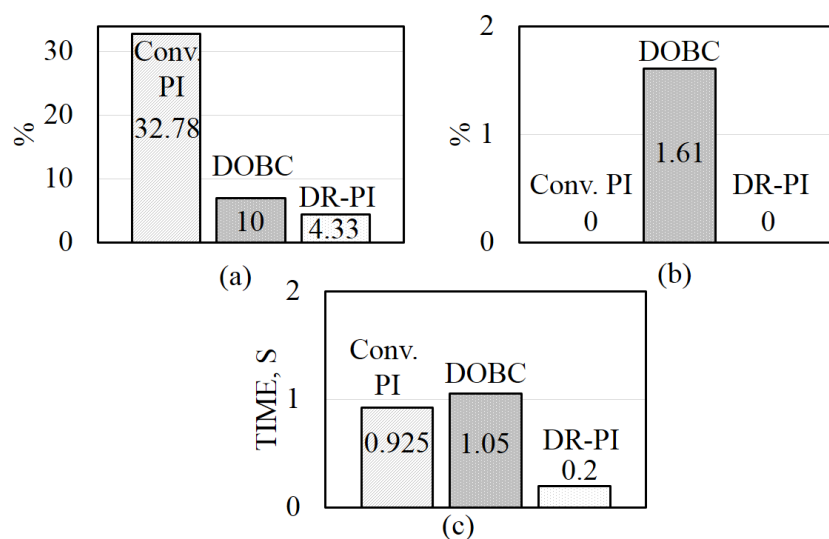


Figure 17. Numerical performance of three control methods under Scenario 2: (a) speed drop; (b) speed overshoot; and (c) settling time.

5. Conclusions

A novel DR-PI controller was proposed and successfully applied to control the speed of PMSMs. The experiments were completed to compare the results of the DR-PI with conventional PI and DOBC schemes. Based on the obtained experimental results, it is obvious that, under a sudden disturbance effect and speed changes, the DR-PI scheme can show superior results with less settling time and absence of overshoot which are common to the two other controllers. Furthermore, unlike the DOBC, in which the PI controller and observer parameters are tuned separately, in the DR-PI controller, the tuning of the PI controller is successfully achieved in close relationship with the tuning of the Q-filter required for disturbance attenuation. Hence, the tuning process of the whole control system becomes more systematic and practical. Thanks to the introduction of the desired closed loop model, the requirement for available plant information (used in DOBC) might be removed. The proposed controller is simple and it has an easy and clear way of tuning the gains. As the experiments show, the controller can be successfully utilized in the control of AC electrical drives, particularly PMSMs. Moreover, the proposed DR-PI controller can be used to replace the conventional PI controller in other applications, but of course, with careful consideration. In this work, we aimed to propose the DR-PI controller which can be tuned in a systematic way and at the same time, with improved performance compared to the conventional PI controller. The advantage of using the DR-PI is that this method does not require exact plant model information to design DOBC scheme. Furthermore, by tuning the controller gains, we are simultaneously able to tune the low-pass filter, which is essential in the suppression of disturbance in the system. However, its drawback is that, unlike the conventional PI, the DR-PI shows a slightly slower response time due to the implicit disturbance estimation mechanism in its design. However, this drawback can be eliminated by carefully designing the pre-filter. The analysis of the relation between the time constants of a desired closed loop model, low-pass filter as well as a compensator and their effect on system performance needs to be considered as a future work.

Author Contributions: Conceptualization, K.S. and T.D.D.; methodology, K.S. and T.D.D.; software, K.S.; validation, K.S. and T.D.D.; formal analysis, K.S. and T.D.D.; investigation, K.S. and T.D.D.; resources, T.D.D.; data curation, K.S. and T.D.D.; writing—original draft preparation, K.S.; writing—review and editing, T.D.D.; visualization, K.S. and T.D.D.; supervision, T.D.D.; project administration, T.D.D.; funding acquisition, T.D.D. All authors have read and agreed to the published version of the manuscript.

Funding: This work was supported by Nazarbayev University under the Faculty Development Competitive Research Grant Program (FDCRGP), Grant No. 11022021FD2924.

Institutional Review Board Statement: Not applicable.

Informed Consent Statement: Not applicable.

Data Availability Statement: Not applicable.

Conflicts of Interest: The authors declare no conflict of interest.

References

1. Kim, J.; Ryu, S.W.; Rifaq, M.S.; Choi, H.H.; Jung, J.E. Improved torque ripple minimization technique with enhanced efficiency for surface-mounted pmsm drives. *IEEE Access* **2020**, *8*, 115017–115027. [[CrossRef](#)]
2. Shi, T.; Yan, Y.; Zhou, Z.; Xiao, M.; Xia, C. Linear quadratic regulator control for PMSM drive systems using nonlinear disturbance observer. *IEEE Trans. Power Electron.* **2019**, *35*, 5093–5101. [[CrossRef](#)]
3. Aghili, F. Optimal feedback linearization control of interior PM synchronous motors subject to time-varying operation conditions minimizing power loss. *IEEE Trans. Ind. Electron.* **2017**, *65*, 5414–5421. [[CrossRef](#)]
4. Song, Y.; Xia, Y.; Wang, J.; Li, J.; Wang, C.; Han, Y.; Xiao, K. Barrier Lyapunov function-based adaptive prescribed performance control of the PMSM used in robots with full-state and input constraints. *J. Vib. Control* **2022**. [[CrossRef](#)]
5. Chen, Z.H.; Xu, Z.D.; Lu, H.F.; Yang, J.Z.; Yu, D.Y.; Zhu, C.; Zhen, S.C.; Zheng, H.M. A new robust control strategy for axial flux permanent magnet motor applied on legged lunar robots. *J. Vib. Control* **2021**. [[CrossRef](#)]
6. Suleimenov, K.; Do, T.D. Design and Analysis of a Generalized High-Order Disturbance Observer for PMSMs With a Fuzzy-PI Speed Controller. *IEEE Access* **2022**, *10*, 42252–42260. [[CrossRef](#)]
7. Rassõlkin, A.; Kallaste, A.; Orlova, S.; Gevorkov, L.; Vaimann, T.; Belahcen, A. Re-use and recycling of different electrical machines. *Latv. J. Phys. Tech. Sci.* **2018**, *55*, 13–23. [[CrossRef](#)]
8. Xia, C.; Liu, N.; Zhou, Z.; Yan, Y.; Shi, T. Steady-state performance improvement for LQR-based PMSM drives. *IEEE Trans. Power Electron.* **2018**, *33*, 10622–10632. [[CrossRef](#)]
9. Choi, J.W.; Lee, S.C. Antiwindup strategy for PI-type speed controller. *IEEE Trans. Ind. Electron.* **2009**, *56*, 2039–2046. [[CrossRef](#)]
10. Errouissi, R.; Al-Durra, A.; Mueen, S.M. Experimental validation of a novel PI speed controller for AC motor drives with improved transient performances. *IEEE Trans. Control Syst. Technol.* **2017**, *26*, 1414–1421. [[CrossRef](#)]
11. Sant, A.V.; Rajagopal, K.R.; Sheth, N.K. Permanent magnet synchronous motor drive using hybrid PI speed controller with inherent and noninherent switching functions. *IEEE Trans. Magn.* **2011**, *47*, 4088–4091. [[CrossRef](#)]
12. Nie, Z.Y.; Zhu, C.; Wang, Q.C.; Gao, Z.; Shao, H.; Luo, J.L. Design, analysis and application of a new disturbance rejection PID for uncertain systems. *ISA Trans.* **2020**, *101*, 281–294. [[CrossRef](#)]
13. Nie, Z.Y.; Li, Z.; Wang, Q.G.; Gao, Z.; Luo, J. A unifying Ziegler–Nichols tuning method based on active disturbance rejection. *Int. J. Robust Nonlinear Control* **2021**. [[CrossRef](#)] [[PubMed](#)]
14. Lin, P.; Wu, Z.; Liu, K.Z.; Sun, X.M. A class of linear-nonlinear switching active disturbance rejection speed and current controllers for PMSM. *IEEE Trans. Power Electron.* **2021**, *36*, 14366–14382. [[CrossRef](#)]
15. Dai, C.; Guo, T.; Yang, J.; Li, S. A disturbance observer-based current-constrained controller for speed regulation of PMSM systems subject to unmatched disturbances. *IEEE Trans. Ind. Electron.* **2020**, *68*, 767–775. [[CrossRef](#)]
16. Rifaq, M.S.; Nguyen, A.T.; Choi, H.H.; Jung, J.W. A robust high-order disturbance observer design for SDRE-based suboptimal speed controller of interior PMSM drives. *IEEE Access* **2019**, *7*, 165671–165683. [[CrossRef](#)]
17. Qu, L.; Qiao, W.; Qu, L. An enhanced linear active disturbance rejection rotor position sensorless control for permanent magnet synchronous motors. *IEEE Trans. Power Electron.* **2019**, *35*, 6175–6184. [[CrossRef](#)]
18. Chen, Q.; Tan, Y.; Li, J.; Mareels, I. Decentralized PID control design for magnetic levitation systems using extremum seeking. *IEEE Access* **2017**, *6*, 3059–3067. [[CrossRef](#)]
19. Meng, F.; Liu, S.; Liu, K. Design of an optimal fractional order PID for constant tension control system. *IEEE Access* **2020**, *8*, 58933–58939. [[CrossRef](#)]
20. Apte, A.; Thakar, U.; Joshi, V. Disturbance observer based speed control of PMSM using fractional order PI controller. *IEEE CAA J. Autom. Sin.* **2019**, *6*, 316–326. [[CrossRef](#)]
21. Liu, Y.; Gao, J.; Zhong, Y.; Zhang, L. Extended state observer-based IMC-PID tracking control of pmsm servo systems. *IEEE Access* **2021**, *9*, 49036–49046. [[CrossRef](#)]
22. Hao, Z.; Yang, Y.; Gong, Y.; Hao, Z.; Zhang, C.; Song, H.; Zhang, J. Linear/nonlinear active disturbance rejection switching control for permanent magnet synchronous motors. *IEEE Trans. Power Electron.* **2021**, *36*, 9334–9347. [[CrossRef](#)]
23. Yan, Y.; Yang, J.; Sun, Z.; Zhang, C.; Li, S.; Yu, H. Robust speed regulation for PMSM servo system with multiple sources of disturbances via an augmented disturbance observer. *IEEE ASME Trans. Mechatronics* **2018**, *23*, 769–780. [[CrossRef](#)]
24. Kuang, Z.; Du, B.; Cui, S.; Chan, C.C. Speed control of load torque feedforward compensation based on linear active disturbance rejection for five-phase PMSM. *IEEE Access* **2019**, *7*, 159787–159796. [[CrossRef](#)]
25. Alfahaid, A.A.; Strangas, E.G.; Khalil, H.K. Speed control of permanent magnet synchronous motor with uncertain parameters and unknown disturbance. *IEEE Trans. Control Syst. Technol.* **2020**, *29*, 2639–2646. [[CrossRef](#)]
26. Lv, H.; Zhang, L.; Yao, C.; Sun, Q.; Du, J.; Chen, X. An Improved Permanent Magnet Synchronous Motor Rotor Position Observer Design Based on Error Harmonic Elimination. *Machines* **2022**, *10*, 633. [[CrossRef](#)]

27. Zhao, M.; An, Q.; Chen, C.; Cao, F.; Li, S. Observer Based Improved Position Estimation in Field-Oriented Controlled PMSM with Misplaced Hall-Effect Sensors. *Energies* **2022**, *15*, 5985. [[CrossRef](#)]
28. Che, Z.; Yu, H.; Mobayen, S.; Ali, M.; Yang, C.; Bartoszewicz, A. An Improved Extended State Observer-Based Composite Nonlinear Control for Permanent Magnet Synchronous Motor Speed Regulation Systems. *Energies* **2022**, *15*, 5699. [[CrossRef](#)]
29. Wang, J. Fuzzy Adaptive Repetitive Control for Periodic Disturbance with Its Application to High Performance Permanent Magnet Synchronous Motor Speed Servo Systems. *Entropy* **2016**, *18*, 261. [[CrossRef](#)]
30. Hicham, F.; Yousfi, D.; Youness, A.D.; Larbi, E.M.; Rahim, N.A. Sliding-Mode Speed Control of PMSM with Fuzzy-Logic Chattering Minimization—Design and Implementation. *Information* **2015**, *6*, 432–442. [[CrossRef](#)]
31. Cui, P.; Zheng, F.; Zhou, X.; Li, W. Current harmonic suppression for permanent magnet synchronous motor based on phase compensation resonant controller. *J. Vib. Control* **2020**, *28*, 735–744. [[CrossRef](#)]
32. Rongyun, Z.; Changfu, G.; Peicheng, S.; Linfeng, Z.; Changsheng, Z. Research on chaos control of permanent magnet synchronous motor based on the synthetical sliding mode control of inverse system decoupling. *J. Vib. Control* **2020**, *27*, 1009–1019. [[CrossRef](#)]
33. Nie, Z.Y.; Wang, Q.G.; She, J.; Liu, R.J.; Guo, D.S. New results on the robust stability of control systems with a generalized disturbance observer. *Asian J. Control* **2019**, *22*, 2463–2475. [[CrossRef](#)]
34. Errouissi, R.; Ouhrouche, M.; Chen, W.H.; Trzynadlowski, A.M. Robust cascaded nonlinear predictive control of a permanent magnet synchronous motor with antiwindup compensator. *IEEE Trans. Ind. Electron.* **2011**, *59*, 3078–3088. [[CrossRef](#)]
35. Liu, L.; Leonhardt, S.; Misgeld, B.J. Design and control of a mechanical rotary variable impedance actuator. *Mechatronics* **2016**, *39*, 226–236. [[CrossRef](#)]
36. Oliveira, P.M.; Vrančić, D. Underdamped second-order systems overshoot control. *IFAC Proc. Vol.* **2012**, *45*, 518–523. [[CrossRef](#)]
37. Singh, N.; Pratap, B.; Swarup, A. Design of robust control for wind turbine using quantitative feedback theory. *IFAC Pap. Online* **2016**, *49*, 718–723. [[CrossRef](#)]
38. Vogt, P.; Lenz, E.; Klug, A.; Westerfeld, H.; Konigorski, U. Robust Two-Degree-of-Freedom Wheel Slip Controller Structure for Anti-lock Braking. *IFAC Pap. Online* **2019**, *52*, 431–437. [[CrossRef](#)]
39. Aguilar-Orduña, M.A.; Zurita-Bustamante, E.W.; Sira-Ramírez, H.; Gao, Z. Disturbance observer based control design via active disturbance rejection control: A PMSM example. *IFAC Pap. Online* **2020**, *53*, 1343–1348. [[CrossRef](#)]